Regular Article

PHYSICAL CHEMISTRY RESEARCH
Published by the
Iranian Chemical Society
www.physchemres.org
info@physchemres.org

***Phys. Chem. Res.**, Vol. 7, No. 4, 785-797, December 2019*
DOI: 10.22036/pcr.2019.173414.1602

Ortho-phenylenediamine Based Bis-ureas as the Ion Selective Sensors; A QM/MD Study

M. Khavani and M. Izadyar*

Computational Chemistry Laboratory, Department of Chemistry, Faculty of Science, Ferdowsi University of Mashhad, Mashhad, Iran

(Received 28 February 2019, Accepted 13 September 2019)

Density functional theory dispersion corrected (DFT-D3) calculations and molecular dynamic (MD) simulations were applied to investigate the sensing ability of four types of receptors (RCs) composed of ortho-phenylenediamine based bis-ureas for selective complexation with the anions, such as Cl^-, Br^-, OAC^-, $PhCO_2^-$, $H_2PO_4^-$ and HSO_4^- in the gas phase and DMSO. On the basis of the data obtained from B3LYP-D3/6-31G+(d,p) calculations, RCs-OAC^- complexes have the maximum binding energy which are reduced in the presence of DMSO as the solvent. IR vibrational frequencies of the RCs' N-H bonds showed a red-shift due to their interactions with the anions in the corresponding complexes. Moreover, HOMO-LUMO analysis indicates that ionization potential (IP) and electron affinity (EA) values decrease, due to the complexation process, which confirms the electron migration from the anions to the RCs. Natural bond orbital (NBO) analysis indicates that charge transfer occurs from the anions to the RCs due to an n-type mechanism and in comparison to other ions, OAC^- has the stronger orbital interactions with the RCs. The 20 ns MD simulations in DMSO show the specific interactions between OAC^- and RC4 confirming the ability of RC4 as a good candidate to be applied as an anion-selective sensor.

Keywords: Ion selective, Molecular dynamic, Electrostatic interaction, Charge transfer, Sensor

INTRODUCTION

Research on the complexation of anions is an area of the academic interest, from the application viewpoint [1]. Because of their roles in many biological and environmental phenomena, the branch of anion sensing and detection by natural and synthetic molecular receptors has become one of the most important fields of supramolecular chemistry [2-5]. Also non-covalent interactions are of great importance in most of the synthetic receptors reported in the fields of physics, chemistry, biology, nanochemistry, and supramolecular chemistry for ion sensing and selective complexation [6-9]. A kind of non-covalent interaction is the hydrogen bond (H-bond) which has extensive applications for ion sensing, due to its ability in selective complex formation [6]. In most of the receptors reported, N-H groups and anions are known as the H-bond donors and H-bond acceptors, respectively [10,11].

There are many reports available on the anion sensing in the literature for the past two decades, especially on the H-bond interaction as a driving force of the selective complex formation [6,12]. Maeda and coworkers, reported a synthetic anion (F^-, Cl^- and $H_2PO_4^-$) receptor based on the H-bond formation, composed of pyrrole and alkene [12]. On the basis of their experimental studies, $H_2PO_4^-$ forms a more stable complex with the receptor in comparison to the other anions.

A receptor based on squaramide and 4-nitrophenyl was proposed by Fabbrizzi group for halide sensing (Cl^-, Br^- and I^-) and oxoanions (NO_3^-, NO_2^-, HSO_4^- and $H_2PO_4^-$) in CH_3CN [13]. The UV-Vis and NMR studies confirmed the H-bond complex formation and F^- makes the most stable complex with the receptor. Beer and coworkers introduced a receptor for the detection of Cl^- and Br^-, constructed from triazolium and rotenone [14]. On the basis of the Beer results, synthetic receptor forms a stable complex with Br^-

*Corresponding author. E-mail: izadyar@um.ac.ir

and Cl^- in the solvent mixture, having an association constant of 970 and 90, respectively. Kim and his colleagues reported an imidazolium-based receptor for anion binding [15]. Spectroscopic methods reveal that this receptor is able to detect $H_2PO_4^-$ in CH_3CN as the solvent in the presence of other anions such as F^-, HSO_4^- and OAC^-.

In our previous study, by employing the theoretical methods, such as density functional theory and molecular dynamic simulation, we investigated the ability of the hybrid cyclic nanopeptides based on the thiourea cryptands for OAC^-, NO_3^-, HSO_4^-, F^-, Cl^- and Br^- sensing in the gas phase and DMSO [16]. The results indicated that these structures form a stable complex with F^- in comparison to other ions. Quantum theory of atoms in molecules (QTAIM) analysis showed that non-covalent interactions, especially H-bond and dispersion interactions are the most important driving forces of the complex formation.

In this research, four different *ortho*-phenylenediamine based bis-ureas as the receptors (Scheme 1) were considered for the detection of Br^-, Cl^-, OAC^-, $PhCO_2^-$, $H_2PO_4^-$ and HSO_4^- in the gas phase and DMSO. Density functional theory dispersion corrected (DFT-D3) calculations were performed to determine the response mechanism and the ability of these RCs to be used as the ion-selective sensors. Moreover, by applying the molecular dynamic (MD) simulations, the competition of different RCs in the complex formation with the anions in the DMSO was investigated.

Receptors for carboxylate anions are important for the recognition of a variety of biomolecules and amino acids. Many of the carboxylate binding sites in these systems contain urea or thiourea groups and many receptors, containing either one or two units of these moieties, are excellent carboxylate receptors and sensors. In order to have a molecular insight into the sensing process, different quantum chemistry descriptors were calculated and discussed to determine the nature of interaction between the different ions and RCs. Finally, to determine the electronic charge transfer and the nature of the interactions between the RCs and anions, QTAIM and natural bond orbital (NBO) analyses were performed. The importance of this work is the comparison of different *ortho*-phenylenediamine based bis-urea receptors in the anion detection in the gas phase and DMSO. Moreover, determination of the nature of the effective forces in the selective complex formation is of importance, too.

THEORETICAL METHODS

DFT-D3 Calculations

The structures of four RCs composed of ortho-phenylenediamine based bis-urea and their complexes with different anions (X = Br^-, Cl^-, OAC^-, $PhCO_2^-$, $H_2PO_4^-$ and HSO_4^-) were optimized by the DFT dispersion corrected method at the B3LYP-D3 level [17]. D3 version of Grimme's dispersion with the original D3 damping function is called the zero-damping version. Also, 6-31+G(d,p) basis set was applied in the gas phase and DMSO [18]. To eliminate the effect of the basis set incompleteness, E_{BSSE} as the basis set superposition error (BSSE) correction was calculated by employing the counterpoise correction method.

In order to have an estimation of the zero-point vibrational energies (ZPVEs) and their thermodynamic parameters during the complex formation, vibrational frequency calculations were performed. On the basis of frequency calculations, the structures having the minimum energy were confirmed by the absence of any imaginary vibrational frequency in the Hessian matrix, and the thermodynamic parameters were calculated by using the Eq. (1).

$$\Delta X_{bin} = X_{complex} - (X_{RCs} + X_{anion}) \quad (1)$$

[X = G (Gibb's free energy), H (enthalpy) and E (energy)]

To investigate the electrostatic interaction and charge transfer between the RCs and different ions, the natural bond orbital analysis was performed [19]. By applying the NBO analysis, donor-acceptor interactions inside the corresponding complexes were fully investigated in the gas phase and DMSO. All calculations were performed by using the Gaussian 09 computational package [20].

Solvation free energies and the effect of DMSO as the solvent on the stability of the complexes were calculated using the conductor like polarizable continuum model (CPCM) [21].

To analyze the nature and strength of interactions

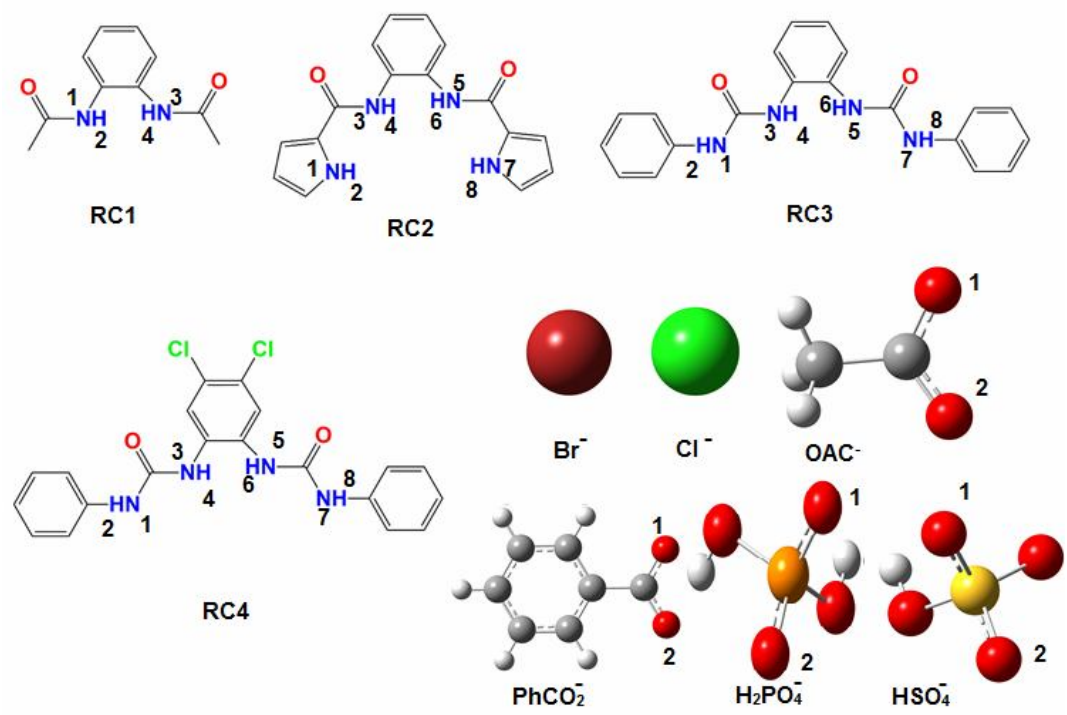

Scheme 1. The studied receptors (RCs) composed of the *ortho*-phenylenediamine based bis-ureas and different anions within atom numbering.

between the ions and RCs, the electron localization function (ELF) [22-26], the localized orbital locator (LOL) [27-30] and QTAIM [31] analyses were performed by MultiWFN 3.1 [32].

Molecular Dynamic Simulations

To investigate the competition of the RCs in the complex formation with the anions, and to analyze the dynamical behavior of the complexes, 20 ns molecular dynamic (MD) simulations were performed in DMSO. In this procedure, the structural parameters of the RCs obtained from the DFT-D3 geometry optimization at the B3LYP-D3/6-31+G(d,p) level and the atomic charges calculated by the CHelpG method at the same level were applied. In the MD simulations, ten molecules of each RC with forty ions were added in a cubic box, randomly. The structures were not closer than 5 Å from each other and Na^+ cation was added to the systems for neutralization. Then, each system was solvated with a cubic box of DMSO so that solvent molecules were located in a distance of 20 Å to the solute molecules. Fox and Kollman parameters were applied in the DMSO simulation [33]. All MD simulations were performed using the Amber 12.0 software [34].

In the first step of MD simulations, 30000-cycle energy minimization was performed on each system. In the next step, by applying an NVT ensemble (with 1000 kJ mol^{-1} nm^{-2} restraining force constant for solute molecules) the systems were heated from 0 to 298.15 K during 1000 ps. The systems were equilibrated without any positional restraint, during 2000 ps in an NPT ensemble (at 298.15 K and 1 atm). Finally, 20 ns MD simulations as the product step were performed on the equilibrated structures with all atoms general amber force field (GAFF) [35].

SHAKE constraints on all bonds involving hydrogen atoms were used with a time step of 2 fs [36]. In order to control the temperature of the systems, a Langevin thermostat [37,38] with a collision frequency of 2 ps^{-1} and 1 ps pressure relaxation time was used in the NPT MD simulations. Particle mesh Ewald (PME) coupled with the periodic boundary conditions with 8 Å direct cut-off was applied to calculate the long-range electrostatic interactions [39].

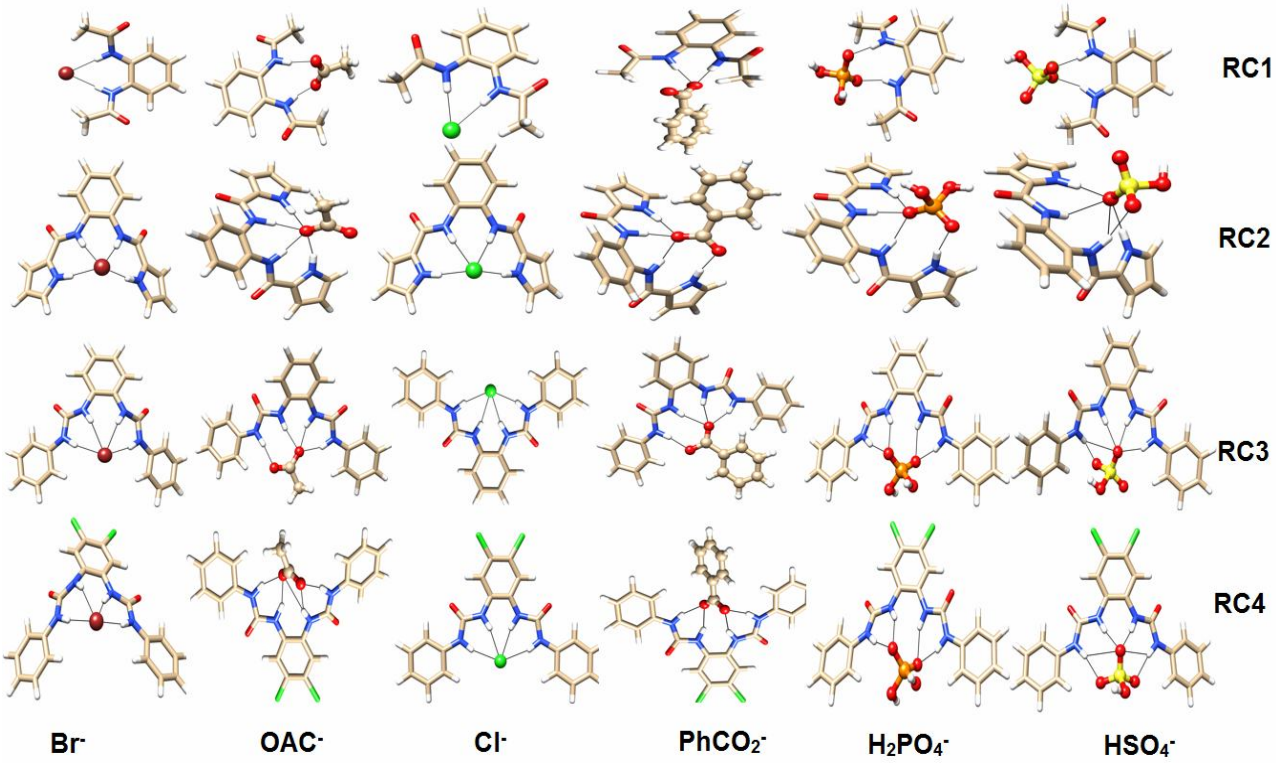

Fig. 1. Optimized structures of the ion-RC complexes in the gas phase.

RESULTS AND DISCUSSION

Structural and IR Vibrational Analysis

The initial structures of the RCs were obtained from the X-ray crystal structures reported by Gale and coworkers [40]. According to Scheme 1, there are two and four N-H groups on the RC1 and other RCs, respectively, which are proper for the H-bond formation with OAC^-, HSO_4^-, $H_2PO_4^-$ and $PhCO_2^-$ and halogen bonds with Cl^- and Br^-.

Figure 1 shows the optimized structures of the ion-RC complexes in the gas phase and the geometrical parameters of the corresponding complexes are reported in Table S1. On the basis of the results, the N-H bond lengths in the RCs increase after complex formation with the different ions. Moreover, the calculated structural parameters of the RCs are in good agreement with the experimental results [40], which are not significantly disturbed in the presence of DMSO.

Structural analysis indicates that the maximum N-H bond lengths of the RC1, RC3 and RC4 are seen in the presence of OAC^-, while in the case of RC2, $PhCO_2^-$ affects this bond more than other anions. The comparison of the optimized structures in DMSO and gas phase, reveals that hydrogen and halogen bond lengths increase in DMSO, which in turn reduces the stability of the ion-RC complexes.

To investigate the RCs response to the different ions, IR vibrational frequencies of the N-H bond of free RCs and RC-ion complexes were calculated and reported in Table S2. There is a significant red-shift in the presence of different ions in both gas phase and DMSO. The quantity of red shift in DMSO is lower than that in the gas phase, confirming a lower stability for ion-RC complexes in DMSO, according to structural analysis.

Binding Energy Analysis

In order to examine the affinity of the RCs to different ions, thermodynamic parameters, such as binding energy (ΔE_{bin}), binding enthalpy (ΔH_{bin}), and binding Gibbs energy (ΔG_{bin}) of the ion-RC complexes were evaluated and reported in Table 1. According to Table 1, the theoretical

Table 1. Calculated Thermodynamic Parameters (kcal mol^{-1}) of the Ion-RC Complexes in the Gas Phase and DMSO

		ΔG_{bin}	ΔH_{bin}	ΔE_{bin}	$\Delta E_{bin+BSSE}$	ΔG_{bin}	ΔH_{bin}	ΔE_{bin}	$\Delta E_{bin+BSSE}$
Ions		RC1				RC2			
Br^-	Gas	-32.68	-42.22	-41.63	-34.96	-47.32	-55.92	-55.33	-43.74
	DMSO	-6.36	-14.19	-13.60	-6.93	-14.07	-22.10	-21.51	-9.92
OAC^-	Gas	-81.94	-45.03	-44.43	-43.23	-44.54	-57.21	-56.62	-56.17
	DMSO	-2.69	-13.80	-13.81	-12.61	-11.85	-21.80	-21.20	-20.75
Cl^-	Gas	-30.82	-39.97	-39.38	-39.16	-42.81	-50.96	-50.37	-49.92
	DMSO	-0.68	-8.30	-7.71	-7.49	-5.27	-12.46	-11.86	-11.41
$PhCO_2^-$	Gas	-28.20	-41.09	-40.49	-39.29	-41.06	-54.53	-53.42	-51.28
	DMSO	-1.09	-14.04	-13.45	-12.25	-10.53	-23.64	-23.05	-20.91
$H_2PO_4^-$	Gas	-24.29	-38.23	-37.63	-35.85	-39.45	-50.97	-50.37	-47.48
	DMSO	-0.65	-11.86	-1.27	0.51	-8.93	-20.86	-20.27	-17.38
HSO_4^-	Gas	-4.52	-13.62	-34.77	-33.17	-30.65	-42.61	-42.02	-39.48
	DMSO	1.92	-10.28	-9.68	-8.08	-5.00	-15.90	-15.31	-12.77
		RC3			RC4				
Br^-	Gas	-44.50	-56.28	-56.28	-44.3	-51.08	-116.48	-59.92	-47.78
	DMSO	-12.30	-21.13	-20.53	-8.55	-13.59	-22.15	-21.56	-9.42
OAC^-	Gas	-45.55	-58.26	-58.26	-56.46	-51.22	-63.94	-63.35	-61.49
	DMSO	-10.57	-21.22	-20.62	-18.82	-12.45	-23.11	-22.52	-20.66
Cl^-	Gas	-43.36	-50.74	-50.74	-50.28	-47.90	-56.29	-55.69	-55.24
	DMSO	-3.92	-11.23	-10.63	-10.17	-5.98	-12.62	-12.03	-11.58
$PhCO_2^-$	Gas	-41.69	-53.98	-53.98	-51.85	-45.91	-60.97	-60.38	-58.26
	DMSO	-10.24	-23.28	-22.69	-20.56	-11.29	-25.73	-25.14	-23.02
$H_2PO_4^-$	Gas	-41.80	-54.09	-54.09	-51.32	-46.55	-59.75	-59.16	-56.31
	DMSO	-6.93	-22.16	-21.57	-18.8	-8.90	-23.88	-23.29	-20.44
HSO_4^-	Gas	-32.35	-44.41	-44.41	-41.79	-38.43	-51.15	-50.56	-47.75
	DMSO	-3.57	-14.26	-13.41	-10.79	-5.54	-17.35	-16.76	-13.95

trend of binding energies is as follows: RC4 > RC3 > RC2 > RC1. On the basis of the calculated ΔE_{bin}, OAC^- forms the most favorable complexes with the studied RCs in the gas phase, which is in contrast to HSO_4^- behavior and in DMSO. $PhCO_2^-$ forms the most stable complexes with RC4 and RC3. Moreover, the binding energies were calculated by using single point energy calculations (Table S3) at the B3LYP-D3/6-311++G(d,p) level of theory, confirming the accuracy of 6-31+G(d,p) basis set. Moreover, the calculated E_{BSSE} values in Table 1 indicate that BSSE has an important effect on the calculated values of ΔE_{bin} for Br^- complexes with different RC, while for other complexes E_{BSSE} has not an important contribution. Also, H-bond interactions in comparison with the halogen bond interactions are more favorable, especially in the gas phase, in agreement with the structural analysis.

A lower sensitivity of the RCs to halide ions in comparison to other ions can be explained by a high electronegativity of Br^- and Cl^-. This property makes them more efficient in electron capture in comparison to the other anions studied. Therefore, halides interact with the H atoms of the N-H groups (of the RCs) weaker than other anions. Negative character of ΔG_{bin} ($\Delta G_{bin} < 0$), of the complex formation process (Table 1) shows that all complexes are favorable, thermodynamically, in the gas phase and DMSO. An unspontaneous nature of the HSO_4^--RC1 complex in DMSO reveals that this complex is not stable, in agreement with the experimental results [40].

Binding enthalpies of the complex formation (ΔH_{bin}) show their exothermic nature in the gas phase and DMSO. Different behaviors of the anions sorption by the RCs in the gas phase and DMSO may be related to a competitive process between the solvent molecules and RCs, in which the solvent molecules are more successful. Therefore, a reduction in the sensitivity of the RCs to the anions is inevitable.

Charge Transfer Mechanism and Donor-acceptor Interaction Analysis

To investigate the charge transfer and donor-acceptor interactions inside the complexes, NBO analysis was performed in the gas phase and DMSO. The stabilization energy E(2), along with the charge transfer, were calculated to determine the p-type and n-type doping mechanisms.

The amount of charge transfer between the ions and RCs were calculated by NBO analysis and reported in Table 2. This Table shows total charges of RCs after response to the anions. According to this table, electronic charges of all RCs are negative, therefore, electrons are transferred from the anions to RCs, indicating an n-type doping mechanism. The maximum values of charge transfer are related to Br^-, Cl^-, OAC^- and $PhCO_2^-$. Moreover, the values of charge transfer reduce significantly in DMSO, which decreases the stability of the corresponding complexes. Table 2 shows that HSO_4^- has the lowest charge transfer to all RCs, which is according to minimum stability of the corresponding complexes.

Table S4, shows all donor-acceptor interactions between the lone pair (Lp) electrons, Lp_O, Lp_{Cl^-} and Lp_{Br^-} as the donors with the antibonding orbital of N-H ($\sigma^*_{N\text{-}H}$) as an acceptor. According to Table S4, donor-acceptor interactions are perturbed in DMSO. This means that some of the donor-acceptor interactions are destroyed completely in DMSO, while some new interactions are created in comparison to the gas phase. For example, the interaction of $Lp_{O1(PhCO2^-)} \rightarrow \sigma^*_{N1\text{-}H2(RC1)}$ is absent in DMSO, while the interaction of $Lp_{O1(PhCO2^-)} \rightarrow \sigma^*_{N5\text{-}H6(RC3)}$ appears only in DMSO.

According to the calculated $\Sigma E(2)$ values (Table 3), OAC^- represents the most orbital interactions, with all RCs in the gas phase and DMSO. In the other words, due to the strong electrostatic orbital interactions, OAC^- forms the most stable complexes with all RCs in comparison to the other ions, according to the structural and energy analyses. On the basis of the NBO analysis, charge transfer and electrostatic interactions between the anions and RCs can be considered as the driving force of the selective complex formation. Moreover, in order to have a better insight on the sensing ability of the corresponding RCs, quantum chemistry reactivity and topological parameters were calculated and reported in supporting information section (Tables S5 and S6).

MD Simulation Results

In order to investigate the time dependent behaviors of the anions in the presence of the RCs, 20 ns

Table 2. Calculated Total Charge Transfer Values of all RCs after Complexation with Different Ions in the Gas Phase and DMSO

Ions		RC1	RC2	RC3	RC4
Br^-	Gas	-0.174	-0.238	-0.208	-0.212
	DMSO	-0.129	-0.198	-0.158	-0.165
OAC^-	Gas	-0.133	-0.183	-0.174	-0.177
	DMSO	-0.132	-0.173	-0.161	-0.169
Cl^-	Gas	-0.169	-0.217	-0.181	-0.189
	DMSO	-0.014	-0.132	-0.174	-0.139
$PhCO_2^-$	Gas	-0.124	-0.189	-0.160	-0.168
	DMSO	-0.123	-0.188	-0.158	-0.167
$H_2PO_4^-$	Gas	-0.093	-0.153	-0.139	-0.143
	DMSO	-0.089	-0.153	-0.134	-0.140
HSO_4^-	Gas	-0.081	-0.128	-0.129	-0.139
	DMSO	-0.070	-0.113	-0.102	-0.129

Table 3. Calculated ΣE(2) Values (kcal mol^{-1}) of all Ion-RC Complexes in the Gas Phase and DMSO

	$Lp_{Br^-} \rightarrow \sigma^*_{N-H}$	$^aLp_O \rightarrow \sigma^*_{N-H}$	$Lp_{Cl^-} \rightarrow \sigma^*_{N-H}$	$^bLp_O \rightarrow \sigma^*_{N-H}$	$^cLp_O \rightarrow \sigma^*_{N-H}$	$^dLp_O \rightarrow \sigma^*_{N-H}$
			RC1			
Gas	31.57	35.19	33.83	29.38	25.38	16.19
DMSO	26.94	34.22	25.76	20.82	24.76	13.69
			RC2			
Gas	37.09	44.80	41.95	43.86	42.34	33.76
DMSO	27.90	35.47	34.05	32.17	32.92	28.00
			RC3			
Gas	33.38	61.66	40.71	46.56	42.33	27.02
DMSO	26.47	25.54	30.14	45.21	38.61	30.93
			RC4			
Gas	36.96	44.82	43.01	43.00	41.05	21.50
DMSO	24.86	43.47	32.38	43.53	39.13	18.99

a, b, c and d are O atoms of OAC^-, $PhCO_2^-$, $H_2PO_4^-$ and HSO_4^- ions, respectively.

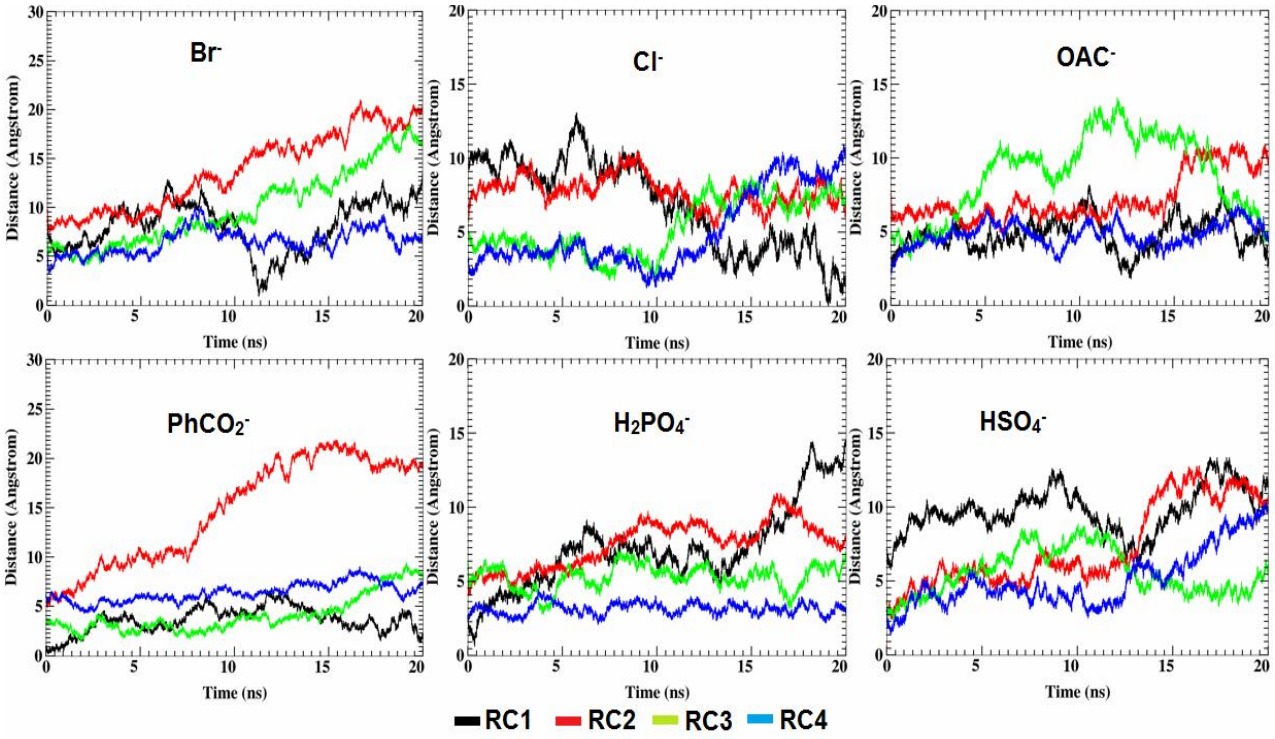

Fig. 2. The calculated distance between the different ions and RCs during the 20 ns MD simulations in DMSO.

Table 4. The Obtained Average Distance, Average Electrostatic Interaction and RDF Distance of the Ion-RC Complexes in the 20 ns MD Simulations in DMSO

	Av. distance (Å)	Av. EIE (kcal mol^{-1})	RDF (Å)	Av. distance (Å)	Av. EIE (kcal mol^{-1})	RDF (Å)	Av. distance (Å)	Av. EIE (kcal mol^{-1})	RDF (Å)
		Br^-			OAC^-			Cl^-	
RC1	8.11	-978.68	1.85	4.81	-14637.30	2.05	6.91	-11325.20	1.85
RC2	13.75	-2426.87	1.95	7.29	-14758.00	2.05	7.78	-10815.70	1.95
RC3	9.94	-4479.66	1.85	8.88	-14340.00	1.85	5.27	-11296.20	1.85
RC4	6.94	-4871.31	1.85	4.79	-14345.60	1.85	5.03	-11262.90	1.85
		$PhCO_2^-$			$H_2PO_4^-$			HSO_4^-	
RC1	3.62	-11654.20	2.15	7.20	-11618.00	2.05	9.73	-8380.07	1.85
RC2	14.73	-11551.10	2.15	7.49	-11967.60	2.15	7.30	-8181.34	1.95
RC3	4.10	-11488.80	1.85	5.29	-12376.90	1.85	5.54	-8248.51	1.85
RC4	6.39	-11551.20	1.85	3.13	-11542.40	1.85	5.08	-8082.61	1.85

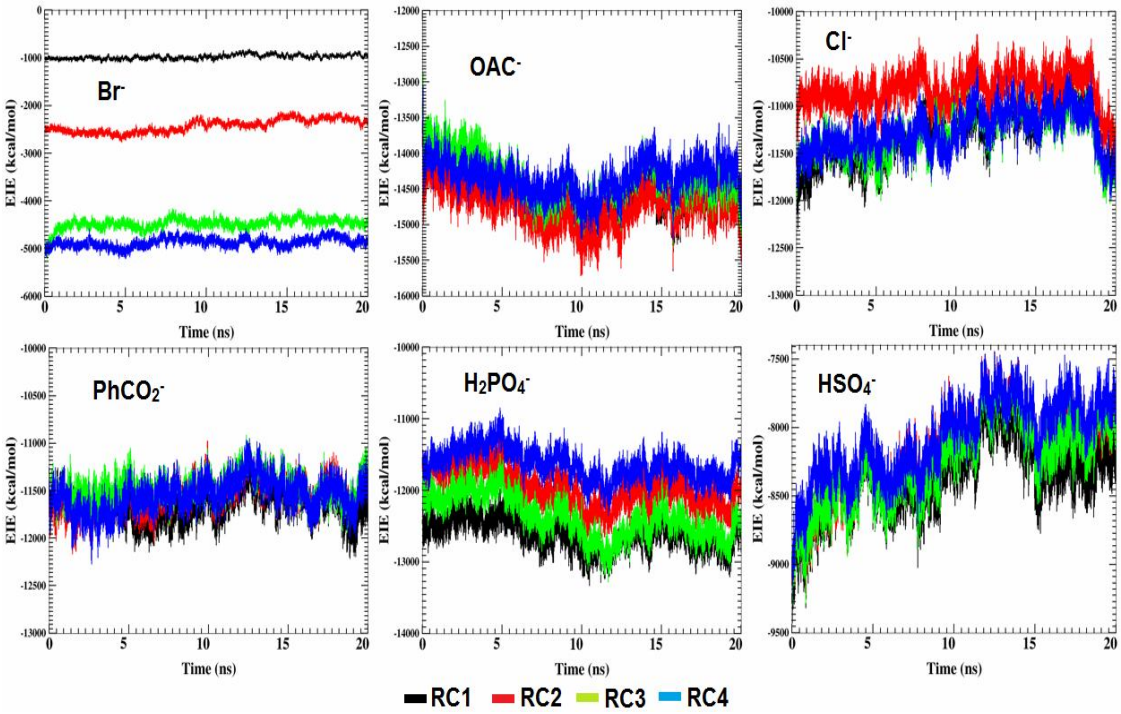

Fig. 3. The calculated electrostatic interaction energy (EIE) (kcal mol^{-1}) between the different anions and RCs during the 20 ns MD simulations.

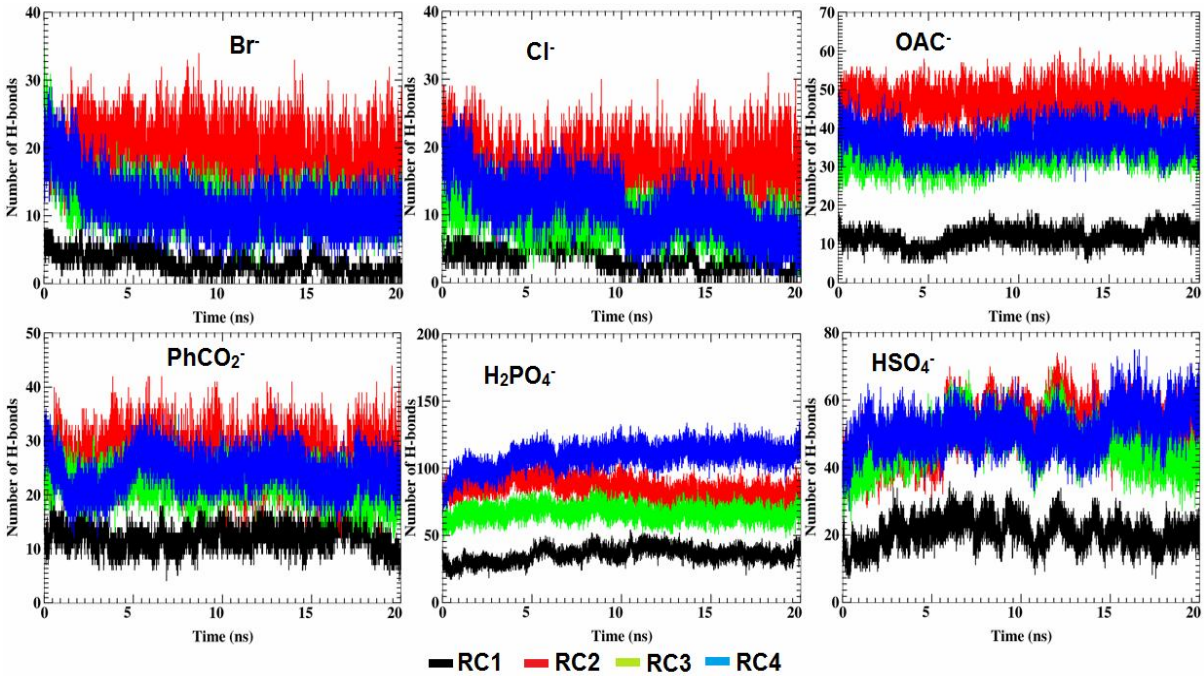

Fig. 4. The calculated number of the H-bonds between the ions and RCs during the 20 ns MD simulations in DMSO.

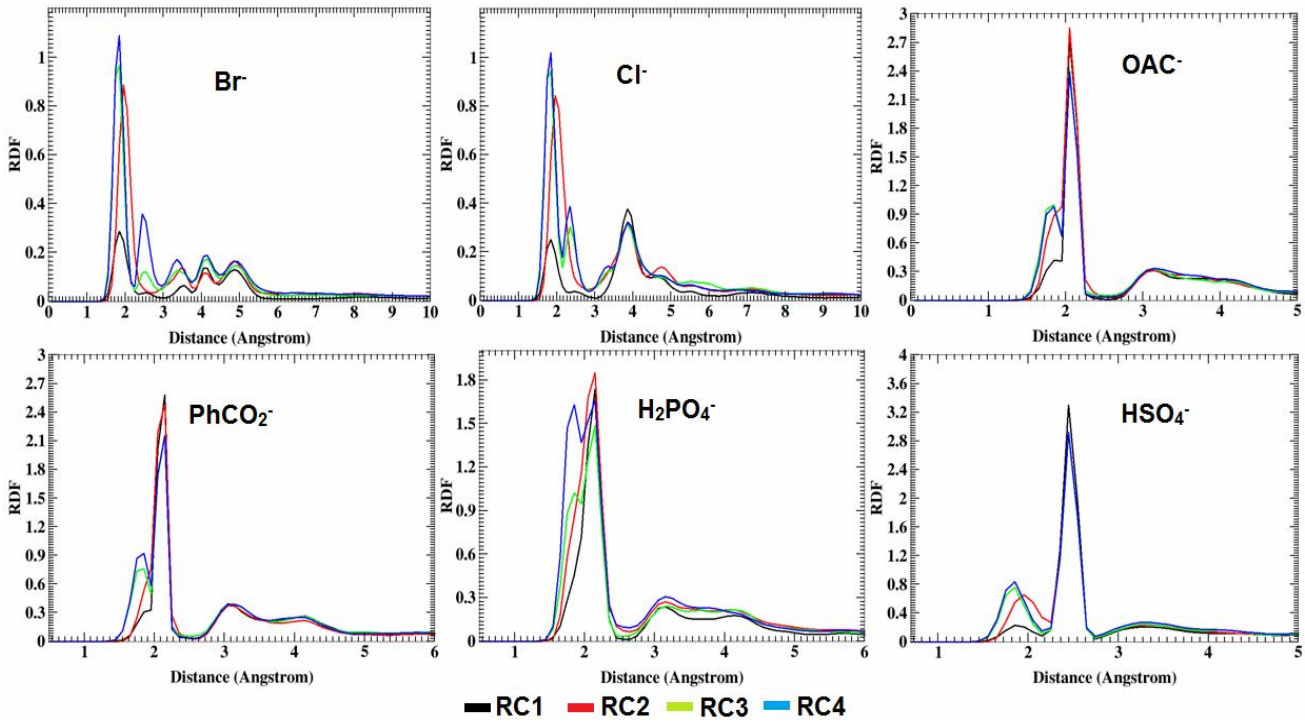

Fig. 5. RDF plots of X⋯H pairs of the ion-RC complexes in DMSO.

MD simulations were performed in DMSO. To do so, 10 molecules of each RC along with 40 anions of each type were added in a cubic box. Figure 2 shows the calculated distances between the anions and RCs during the simulation times. According to this figure, Br^-, OAC^-, Cl^-, $PhCO_2^-$, $H_2PO_4^-$ and HSO_4^- are located at the minimum distance with RC4, RC4, RC4, RC1, RC4 and RC4, respectively. Therefore, RC4 well interacts with the anions in the presence of other RCs, which is in agreement with the DFT-D3 results.

Figure 3 shows the electrostatic interaction energy (EIE) between the anions and RCs. According to this figure and Table 4, the maximum electrostatic interaction energies of Cl^-, $PhCO_2^-$ and HSO_4^- are related to their complexes with the RC1, while for other anions of Br^-, OAC^- and $H_2PO_4^-$, RC4, RC2 and RC3 are the most interactive receptors, respectively.

In agreement with the quantum chemistry calculations, OAC^- makes the most stable complexes with different RCs, based on the EIE analysis of the MD simulation data. The analysis of the H-bond during the complex formation is of importance to have an insight into the intermolecular interaction for prediction of the sensing activity of the chemical receptors. For this purpose, the amount of the H-bonds were determined on the basis of the H-bond fluctuation analysis during the simulation time (Fig. 4).

The minimum number of the H-bonds is observed in the anion-RC1 complexes due to the least amount of the N-H bonds (2N-H bonds). On the other hand, HSO_4^--RC4, $H_2PO_4^-$-RC4 and OAC^--RC2 complexes have the most numbers of H-bonds. This property can be considered as a key parameter in the ion selectivity of the receptors from the molecular viewpoint.

Radial distribution function (RDF) plots, Fig. 5, show the probability of finding the X⋯H pair in the ion-RC complexes. According to Table 4 and Fig. 5, the first sharp peak of the O⋯H pair (O atoms of OAC^-) is located at 1.85 Å in the cases of RC3 and RC4, confirming H-bond formation in the corresponding complexes.

On the basis of the RDF analysis, there is the least possibility for H-bond formation in the $PhCO_2^-$-RC1 and $PhCO_2^-$-RC2 complexes, while a different behavior is

observed in the cases of RC4 and RC3. Moreover, RDF plots indicate that in most cases, RC3 and RC4 interactions with different ions are more considerable in comparison to RC1 and RC2. Finally, MD simulation results in DMSO indicate that the interactions of OAC^- with the RCs are more considerable in comparison to the other ions, making these receptors more favorable in OAC^- sensing. Moreover, RC4 is proposed as a better receptor for the selective complex formation. The MD results are in agreement with the DFT-D3 data.

Conflicts of Interest

There are no conflicts of interest to declare.

ACKNOWLEDGEMENTS

The Research Council of Ferdowsi University of Mashhad is acknowledged for financial support (3/44401). We hereby acknowledge that part of this computation was performed at the HPC center of Ferdowsi University of Mashhad.

CONCLUSIONS

DFT-D3 calculations confirm a red shift in the IR vibrational frequencies of the N-H groups of RCs, after complex formation, in the gas phase and DMSO. During the complex formation, the N-H bond length increases, so that the maximum bond length is observed in the presence of OAC^- in comparison to the other anions. On the basis of the calculated thermodynamic parameters, OAC^- forms the most stable complexes with different RCs in comparison to other ions. Different behaviors of the RCs in confronting with the anions, in the gas phase and DMSO, may be related to a competitive process between the solvent molecules and RCs for anion sensing, in which the solvent molecules are more successful. Therefore, a reduction in the sensitivity of the RCs to the anions is inevitable. NBO and QTAIM analyses confirm that electrostatic interactions and charge transfer between the anions and RCs are the driving forces in the complex formation. There is an n-type mechanism in the charge transfer process. On the basis of the MD simulations in DMSO, the maximum electrostatic interaction energies of the Cl^-, $PhCO_2^-$ and HSO_4^- are related to their complexes with the RC1. Also, RC4, RC2, and RC3 are the most interactive receptors against Br^-, OAC^- and $H_2PO_4^-$, respectively. Finally, on the basis of different analyses, there is a reasonable potential for different RCs to behave selectively against the OAC^-.

SUPPORTING INFORMATION

The calculated geometrical parameters of the ion-RC complexes in the gas phase and DMSO (Table S1), Calculated IR vibration frequencies (cm^{-1}) of the N-H groups of RCs and their complexes in the gas phase and DMSO (Table S2). The calculated ΔE_{bin} of the ion-RC complexes using the B3LYP-D3/6-311++G(d,p) level of theory in the gas phase and DMSO (Table S3), Calculated E(2) values (kcal mol^{-1}) of the ion-RC complexes in the gas phase and DMSO (Table S4), HOMO-LUMO and density of state analyses, Topological analysis, Calculated quantum reactivity indices (a.u.) of the bare RCS and their ion complexes in the gas phase and DMSO (Table S5), Calculated topological parameters (a.u.) of the ion-RC complexes in the gas phase and DMSO (Table S6), DOS spectra of the RCs and their complexes in the gas phase and DMSO (Fig. S1), ELF and LOL plots of the OAC^--RCs complexes in DMSO (Fig. S2), HOMO-LUMO analysis, and Cartesian coordinates of the optimized complexes in the gas phase.

REFERENCES

[1] Busschaert, N.; Caltagirone, C.; Van Rossom, W.; Gale, P. A., Applications of supramolecular anion recognition. *Chem. Rev.* **2015**, *115*, 8038-8155, DOI: 10.1021/acs.chemrev.5b00099.

[2] Evans, N. H.; Beer, P. D., Advances in anion supramolecular chemistry: From recognition to chemical applications. *Angew. Chem. Int. Ed.* **2014**, *53*, 11716-11754, DOI: 10.1002/anie.201309937.

[3] Gale, P. A.; Busschaert, N.; Haynes, C. J.; Karagiannidis, L. E.; Kirby, I. L., Anion receptor chemistry: highlights from 2011 and 2012. *Chem. Soc. Rev.* **2014**, *43*, 205-241, DOI: 10.1039/C3CS60316D.

[4] Santos-Figueroa, L. E.; Moragues, M. E.; Climent, E.;

Agostini, A.; Martínez-Máñez, R.; Sancenón, F., Chromogenic and fluorogenic chemosensors and reagents for anions. A comprehensive review of the years 2010-2011. *Chem. Soc. Rev.* **2013**, *42*, 3489-3613, DOI: 10.1039/C3CS35429F.

[5] Gale, P. A.; Howe, E. N.; Wu, X., Anion receptor chemistry. *Chemistry* **2016**, *1*, 351-422, DOI: 10.1016/j.chempr.2016.08.004.

[6] Scheiner, S., Hydrogen Bonding: A theoretical Perspective. Oxford University Press on Demand, **1997**.

[7] Gale, P. G.; Caltagirone, C., Fluorescent and colorimetric sensors for anionic species, *Coord. Chem. Rev.* **2018**, *354*, 2-27, DOI: 10.1016/j.ccr.2017.05.003.

[8] Gale, P. G.; Caltagirone, C., Chemosensors: Principles, Strategies, and Applications **2011**, 395-427, DOI: 10.1002/9781118019580.ch19.

[9] Brooks, S. J.; Gale, P. A.; Light, M. E., Carboxylate complexation by 1,1′-(1,2-phenylene) bis(3-phenylurea) in solution and the solid state, *Chem. Commun.* **2005**, *37*, 4696-4698, DOI: 10.1039/B508144K.

[10] Brooks, S. J.; Gale, P. A.; Light, M. E., *ortho*-Phenylenediamine bis-urea-carboxylate: A new reliable supramolecular synthon, *Cryst. Eng. Comm.* **2005**, *7*, 586-591. DOI: 10.1039/B511932D.

[11] Molina, P.; Zapata, F.; Caballero, A., Anion recognition strategies based on combined noncovalent interactions, *Chem. Rev.* **2017**, *117*, 9907-9972, DOI: 10.1021/acs.chemrev.6b00814.

[12] Maeda, H.; Kusunose, Y., Dipyrrolyldiketone difluoroboron complexes: Novel anion sensors with C-H· · · X− Interactions. *Chem. Eur. J.* **2005**, *11*, 5661-5666, DOI: 10.1002/chem.200500627.

[13] Amendola, V.; Bergamaschi, G.; Boiocchi, M.; Fabbrizzi, L.; Milani, M., The squaramide versus urea contest for anion recognition. *Chem. Eur. J.* **2010**, *16*, 4368-4380, DOI: 10.1002/chem.200903190.

[14] Mullen, K. M.; Mercurio, J.; Serpell, C. J.; Beer, P. D., Exploiting the 1,2,3-triazolium motif in anion-templated formation of a bromide-selective rotaxane host assembly. *Angew. Chem.* **2009**, *121*, 4875-4878, DOI: 10.1002/anie.201403659.

[15] Jadhav, J. R.; Bae, C. H.; Kim, H. -S., Fluorescence sensing of by a imidazolium-based cholestane receptor. *Tetrahedron Lett.* **2011**, *52*, 1623-1627, DOI: 10.1016/j.tetlet.2011.01.107.

[16] Izadyar, M.; Khavani, M.; Housaindokht, M. R., Sensing ability of hybrid cyclic nanopeptides based on thiourea cryptands for different ions, A joint DFT-D3/MD study. *J. Phys. Chem. A* **2017**, *121*, 244-255, DOI: 10.1021/acs.jpca.6b09738.

[17] Grimme, S.; Antony, J.; Ehrlich, S.; Krieg, H., A consistent and accurate *ab initio* parametrization of density functional dispersion correction (DFT-D) for the 94 elements H-Pu. *J. Chem. Phys.* **2010**, *132*, 154104-154108, DOI: 10.1063/1.3382344.

[18] Bartlett, R. J.; Purvis, G. D., Many-body perturbation theory, coupled-pair many-electron theory, and the importance of quadruple excitations for the correlation problem. *Int. J. Quantum Chem.* **1978**, *14*, 561-581, DOI: 10.1002/qua.560140504.

[19] Reed, A. E.; Curtiss, L. A.; Weinhold, F., Intermolecular interactions from a natural bond orbital, donor-acceptor viewpoint. *Chem. Rev.* **1988**, *88*, 899-926, DOI: 10.1021/cr00088a005.

[20] Frisch, J.; Trucks, G. W.; Schlegel, H. B.; Scuseria, G. E.; Robb, M. A.; Cheeseman, J. R.; Montgomery, J. A.; Vreven, T.; Kudin, K. N.; Burant, C. J.; *et al*., Gaussian 09; Gaussian, Inc.: Pittsburgh, P. A., **2009**.

[21] Cossi, M.; Barone, V.; Cammi, R.; Tomasi, J., *Ab initio* study of solvated molecules: A new implementation of the polarizable continuum model. *Chem. Phys. Lett.* **1996**, *255*, 327-335, DOI: 10.1021/ja0259584.

[22] Scherer, W.; Sirsch, P.; Shorokhov, D.; Tafipolsky, M.; McGrady, G. S.; Gullo, E., Valence charge concentrations, electron delocalization and β-agostic bonding in d0 metal alkyl complexes. *Chem. Eur. J.* **2003**, *9*, 6057-6070, DOI: 10.1002/chem.200304909.

[23] Shurki, A.; Hiberty, P. C.; Shaik, S., Charge-shift bonding in group IVB halides: a valence bond study of MH_3-Cl (M = C, Si, Ge, Sn, Pb) molecules. *J. Am. Chem. Soc.* **1999**, *121*, 822-834, DOI: 10.1021/ja982218f.

[24] Becke, A. D.; Edgecombe, K. E., A simple measure of electron localization in atomic and molecular systems.

J. Chem. Phys. **1990**, *92*, 5397-5403, DOI: 10.1021/ja982218f.

[25] Savin, A.; Nesper, R.; Wengert, S.; Fässler, T. F., ELF: The electron localization function. *Angew. Chem. Int. Ed.* **1997**, *36*, 1808-1832, DOI: 10.1002/anie.199718081.

[26] Burdett, J. K.; McCormick, T. A., Electron localization in molecules and solids: the meaning of ELF. *J. Phys. Chem. A.* **1998**, *102*, 6366-6372, DOI: 10.1021/jp9820774.

[27] Savin, A.; Jepsen, O.; Flad, J.; Andersen, O. K.; Preuss, H.; von Schnering, H. G., Electron localization in solid-state structures of the elements: the diamond structure. *Angew. Chem. Int. Ed.* **1992**, *31*, 187-188, DOI: 10.1002/anie.199201871.

[28] Tsirelson, V.; Stash, A., Determination of the electron localization function from electron density. *Chem. Phys. Lett.* **2002**, *351*, 142-148, DOI: 10.1016/S0009-2614(01)01361-6.

[29] Schmider, H.; Becke, A., Chemical content of the kinetic energy density. *J. Mol. Struc. THEOCHEM.* **2000**, *52*, 51-61, DOI: 10.1016/S0166-1280(00)00477-2.

[30] Jacobsen, H., Localized-orbital locator (LOL) profiles of chemical bonding. *Can. J. Chem.* **2008**, *86*, 695-702, DOI: /10.1139/v08-052.

[31] Schmidt, M. W.; Baldridge, K. K.; Boatz, J. A.; Elbert, S. T.; Gordon, M. S.; Jensen, J. H.; Koseki, S.; Matsunaga, N.; Nguyen, K. A.; Su, S., General atomic and molecular electronic structure system. *J. Comput. Chem.* **1993**, *14*, 1347-1363, DOI: 10.1002/jcc.540141112.

[32] Lu, T.; Chen, F., Multiwfn: A multifunctional wavefunction analyzer. *J. Comput. Chem.* **2012**, *33*, 580-592, DOI: 10.1002/jcc.22885.

[33] Fox, T.; Kollman, P. A., Application of the RESP methodology in the parametrization of organic solvents. *J. Phys. Chem. B.* **1998**, *102*, 8070-8079, DOI: 10.1021/jp9717655.

[34] Case, D. A.; Darden, T.; Cheatham, T.; Simmerling, C. L.; Wang, J.; Duke, R. E.; Luo, R.; Crowley, M.; Walker, R. C.; Zhang, W., Amber 10; University of California, **2008**.

[35] Dickson, C. J.; Rosso, L.; Betz, R. M.; Walker, R. C.; Gould, I. R., GAFFlipid: A general amber force field for the accurate molecular dynamics simulation of phospholipid. *Soft Matter.* **2012**, *8*, 9617-9627, DOI: 10.1039/C2SM26007G.

[36] Ryckaert, J.-P.; Ciccotti, G.; Berendsen, H. J., Numerical integration of the cartesian equations of motion of a system with constraints: molecular dynamics of n-alkanes. *J. Comput. Phys.* **1977**, *23*, 327-341, DOI: 10.1016/0021-9991(77)90098-5.

[37] Uberuaga, B. P.; Anghel, M.; Voter, A. F., Synchronization of trajectories in canonical molecular-dynamics simulations: Observation, explanation, and exploitation. *J. Chem. Phys.* **2004**, *120*, 6363-6374, DOI: 10.1063/1.1667473.

[38] Sindhikara, D. J.; Kim, S.; Voter, A. F.; Roitberg, A. E., Bad seeds sprout perilous dynamics: Stochastic thermostat induced trajectory synchronization in biomolecules. *J. Chem. Theory Comput.* **2009**, *5*, 1624-1631, DOI: 10.1021/ct800573m.

[39] Berne, B. J.; Straub, J. E., Novel methods of sampling phase space in the simulation of biological systems. *Curr. Opin. Struct. Biol.* **1997**, *7*, 181-189, DOI: 10.1016/S0959-440X(97)80023-1.

[40] Brooks, S. J.; Edwards, P. R.; Gale, P. A.; Light, M. E., Carboxylate complexation by a family of easy-to-make *ortho*-phenylenediamine based bis-ureas: studies in solution and the solid state. *New J. Chem.* **2006**, *30*, 65-70, DOI: 10.1039/B511963D.